Ab initio calculations of g_j factors for Li, Be^+, and Ba^+

E. Lindroth* and A.Ynnerman†
Department of Physics, Chalmers University of Technology, 412 96 Göteborg, Sweden
(Received 5 March 1992)

Atomic g_j factors have been calculated for Li, Be^+, and Ba^+ with accurate relativistic wave functions obtained in the coupled-cluster single- and double-excitation approximation. Correlation due to the Coulomb as well as the Breit interaction is included. The results are $-2.002\,301\,58(20)$, $-2.002\,262\,77(50)$, and $-2.002\,491\,1(30)$ for Li, Be^+, and Ba^+, respectively, which agree well with the experimental results $-2.002\,301\,00(64)$, $-2.002\,262\,36(33)$, and $-2.002\,490\,6(12)$. The inclusion of the Breit interaction in the wave functions gives significant contributions to the final results.

Pacs number(s): 31.30.Jv, 31.20.Di, 31.20.Tz, 32.60.+i

I. INTRODUCTION

The development during recent years of sophisticated relativistic methods for many-body systems has given new tools for the treatment of various atomic properties. Among these is the study of the deviation of the magnetic moment for a bound $S_{1/2}$ system from that of a free electron. This property is of special interest since it is of completely relativistic origin and thus is a crucial test of the ability to treat the combination of relativistic and many-body effects.

The study of Zeeman splittings has a long history in precision spectroscopy and due to the recent development of ion-trap techniques experimental g_j factors for ions are now available, including heavy systems as Ba^+ [1, 2] and Hg^+ [3]. Bound-state corrections to the electron g factor have been studied in detail in hydrogen [4, 5] and helium [6, 7] by Grotch and Hegstrom. Expressions for the contributions to the g_j factor in the nonrelativistic limit were given in [6]. In [7] it was demonstrated how the very accurate results obtained by Pekeris could be employed directly to give an essentially exact value for the helium g_j factor, including nuclear-mass corrections and bound-state radiative effects. Lithium has been treated by Hegstrom [8] and Veseth [9, 10]. These calculations were performed in the nonrelativistic limit and in Refs. [8, 9] the effect of correlation in the wave functions was neglected. In Ref. [9] Veseth treated all the first-row elements as well as sodium in the framework of spin extended Hartree-Fock theory. This method includes polarization but neglects correlation. In the later work [10] many-body perturbation theory was applied to the alkali metals up to rubidium and to the first-row elements. All third-order contributions, two orders in the Coulomb interaction and one order in the magnetic perturbation, and some fourth-order contributions were included. Dzuba *et al.* have made relativistic calculations on some heavy elements [11], where spin-polarization effects are accounted for. In a very recent calculation on lead and bismuth [12], second-order correlation, and some classes of higher-order correlation were also included.

A careful treatment in the nonrelativistic limit can usually provide very good results for light systems even when, as in the case of bound-state corrections to the g_j factor, the studied property is a completely relativistic phenomenon. Nevertheless, a relativistic formalism should be employed for heavier systems. As pointed out by Flambaum, Khriplovich, and Sushkov [13] important contributions to the Cs g_j factor arise from terms which in a nonrelativistic formalism, where the spin-orbit interaction is included to lowest order only, would cancel exactly. As discussed by Veseth [10], in connection with his rubidium calculation, the difficulties to account completely for the departure from LS coupling may also constitute a severe problem for heavy systems. The nonrelativistic treatment, which even without these considerations includes a number of cumbersome operators, will then pass the limit where it can be used conveniently.

In the present work we have applied a fully relativistic treatment to a few systems. The g_j factors have been calculated with all order-correlated wave functions obtained in the coupled-cluster single- and double-excitation (CCSD) scheme implemented by Salomonson and Öster [14]. As described in Refs. [15, 16] the diagonalization of a discretized one-particle Hamiltonian yields a finite discrete basis set which is used to solve the coupled equations in the CCSD method. The method used to obtain a finite single-particle spectrum has similarities to the B-spline method devolped by Johnson, Blundell, and Sapirstein [17]. The many-body treatment used here has previously been applied nonrelativistically to study properties such as hyperfine structure, isotope shifts, and transition probabilities in Li [18], Na[19], and K[20]. These represent the most recent extensions of the coupled-cluster approach developed by Lindgren and coworkers [21–23]. The relativistic coupled-cluster scheme has been applied to helium- [16, 24] and berylliumlike systems [25, 26] and in a limited form to parity-violating phenomena, hyperfine structure, and isotope shifts in Cs and Tl [27–29]. Just as in the treatment of the forbidden $M1$ transition $2\,^3S_1$-$1\,^1S_0$ in heliumlike argon [24] it is in the present case necessary to include the effect of the Breit interaction in the wave functions since it affects the

result in leading order.

Here we present calculations on Li, Be^+, and the recently measured ion Ba^+. Section II discusses the relativistic operator for the interaction with a magnetic field and explains how it can be expressed in a convenient form. The correct treatment of negative-energy states is penetrated and finally contributions from the Breit interaction and of radiative origin are discussed. The method of calculation is described in Sec. III and the results are given in Sec. IV.

II. THEORY

The interaction between the atom and a magnetic field is considered through the addition of a term

$$H^m = \sum_i h_i^m = \sum ec\boldsymbol{\alpha}_i \cdot \mathbf{A}_i \tag{1}$$

to the relativistic no-pair Hamiltonian

$$H = \sum_i h_i - e\sum_{i<j} V_{ij} \tag{2}$$

where

$$h = c\boldsymbol{\alpha}\cdot\mathbf{p} + \beta mc^2 - \frac{e^2}{4\pi\epsilon_0}\frac{Z}{r}. \tag{3}$$

The two-particle term V_{ij} includes the Coulomb as well as the Breit interaction surrounded with projection operators onto positive-energy states. The additional contributions from virtuals pairs will be considered in Sec. II A. In Eqs. (1)–(3) radiative effects are omitted. In Sec. II C the extra terms which are added to the interaction term, Eq. (1), as well as to the Hamiltonian without external fields, Eq. (2), when a QED treatment is applied, will be discussed.

If the magnetic field is assumed to be homogeneous over the extension of the atom the vector potential $\mathbf{A}$ can be written

$$\mathbf{A} = -\frac{1}{2}(\mathbf{r}\times\mathbf{B}) \tag{4}$$

and thus

$$h^m = -\frac{ec}{2}(\boldsymbol{\alpha}\times\mathbf{r})\cdot\mathbf{B} = \frac{ec}{2}i\sqrt{2}\,r\left\{\boldsymbol{\alpha}\mathbf{C}^1\right\}^1\cdot\mathbf{B}. \tag{5}$$

Classically the energy for a magnetic dipole in a magnetic field is given as the scalar product between the dipole and the field. The magnetic dipole created by the motion of a charged particle is proportional to its angular momentum and we write

$$E = -\boldsymbol{\mu}\cdot\mathbf{B} = -g_j\frac{e}{2m}\mathbf{j}\cdot\mathbf{B} = -g_j\frac{\mu_B}{\hbar}\mathbf{j}\cdot\mathbf{B} \tag{6}$$

where the g_j factor, with a classical value of -1, has been introduced. Equations (5) and (6) can now be combined to give an expression for the g_j factor:

$$g_j\langle\mathbf{j}\rangle = -\left\langle mc\sqrt{2}\,ir\left\{\boldsymbol{\alpha}\mathbf{C}^1\right\}^1\right\rangle. \tag{7}$$

When Eq. (7) is used the result for a free electron is $g_{\text{Dirac}} = -2$. This is also the bound-state value for an s-electron in the nonrelativistic limit. Corrections to this value have two main sources. First, *radiative* effects, omitted in Eq. (7), give the Schwinger correction of approximately $-0.002\,319$, for a free electron. Second, the expression (7) gives *relativistic* corrections to the g_j factor for a bound electron. These scale as $Z^2\alpha^2$ and are of the order 10^{-4} or 10^{-5} in light systems. Finally, there are also *bound-state radiative corrections*. These are smaller than the *bound-state relativistic corrections* by one order of the fine-structure constant and will be briefly discussed in Sec. II C.

If the expression in Eq. (7) is used directly, together with relativistic wave functions, it will thus give the nonrelativistic factor of -2 and, in addition to that, the bound-state corrections. Due to the relative smallness of these corrections the requirement on the numerical accuracy will be very high. To get three significant figures for the corrections nine significant figures have to be produced. In addition, the absence of nonrelativistic bound-state corrections is not explicit in Eq. (7), but has to be achieved by numerical means. It would certainly be desirable to have an operator which instead gave the corrections directly. To some extent this can be achieved as follows.

When the magnetic Hamiltonian is rewritten as

$$H^m = [P, H] + H^{\text{eff}} \tag{8}$$

an expectation value of H^m between eigenstates of the full Hamiltonian H can be replaced by the expectation value of H^{eff}. Such effective operators have been widely used in connection with parity- and time-reversal violating properties, where they were developed in particular by Sandars [30, 31]. Here a wise choice of the operator P is one that results in an operator H^{eff} which is separable in one part which produce the nonrelativistic value and one part which gives the relativistic bound-state corrections. If P is chosen as

$$P = -\frac{e}{2mc}\sum_i \beta_i\boldsymbol{\alpha}_i\cdot\mathbf{A}_i, \tag{9}$$

the magnetic interaction is readily written as

$$\begin{aligned} h_i^m &= ec\boldsymbol{\alpha}_i\cdot\mathbf{A}_i \\ &= -\frac{e}{2mc}[\beta_i\boldsymbol{\alpha}_i\cdot\mathbf{A}_i, H] + \frac{e}{2m}\beta_i\{\boldsymbol{\sigma}_i\cdot\mathbf{A}_i, \boldsymbol{\sigma}_i\cdot\mathbf{p}_i\} \\ &\quad + \frac{e}{2mc}\left[\beta_i\boldsymbol{\alpha}_i\cdot\mathbf{A}_i, -e\sum_{i<j}V_{ij}\right]. \end{aligned} \tag{10}$$

The last term involves the potential and would be zero for a local Coulomb potential as $V_{ij} = e/(4\pi\epsilon_0 r_{ij})$. However, when the electron-electron interaction is properly surrounded with projection operators, special care has to be taken, as will be discussed below. Further, when the Breit interaction is included in V_{ij} the last term will certainly be nonzero. This will be investigated below as well. The first term on the right-hand side of (10) gives

no contribution to an expectation value and we consider now the second term in (10). If Eq. (4) is used for **A** this term is written

$$\frac{e}{2m}\beta\{\boldsymbol{\sigma}\cdot\mathbf{A},\boldsymbol{\sigma}\cdot\mathbf{p}\}=\frac{e}{2m}\beta(\boldsymbol{l}+\hbar\boldsymbol{\sigma})\cdot\mathbf{B}. \tag{11}$$

The contribution to the value of $g_j\langle\mathbf{j}\rangle$ from this term is thus

$$\langle-\beta(\boldsymbol{l}+\hbar\boldsymbol{\sigma})\rangle=\langle-\beta(2\mathbf{j}-\boldsymbol{l})\rangle \tag{12}$$

as follows from Eq. (6). This operator deviates from the pure nonrelativistic operator only by the presence of the β matrix.

If the expectation value of (12) is taken between single-particle orbitals in any approximation, the nonrelativistic result can easily be separated out:

$$\begin{aligned}\langle\Phi_\kappa\parallel-\beta(2\mathbf{j}-\boldsymbol{l})\parallel\Phi_\kappa\rangle&=-\langle\kappa\parallel 2\mathbf{j}-\boldsymbol{l}\parallel\kappa\rangle\langle f(r)\mid f(r)\rangle+\langle-\kappa\parallel 2\mathbf{j}-\boldsymbol{l}\parallel-\kappa\rangle\langle g(r)\mid g(r)\rangle\\&=-\langle\kappa\parallel 2\mathbf{j}-\boldsymbol{l}\parallel\kappa\rangle+\{\langle\kappa\parallel 2\mathbf{j}-\boldsymbol{l}\parallel\kappa\rangle+\langle-\kappa\parallel 2\mathbf{j}-\boldsymbol{l}\parallel-\kappa\rangle\}\langle g(r)\mid g(r)\rangle.\end{aligned} \tag{13}$$

The fact that the functions Φ are normalized has been used to rewrite the integral over the large components to an integral over the small component plus a pure angular term which gives the nonrelativistic result. Thus the two last terms on the right-hand side of (13) gives the relativistic bound-state correction to the g_j factor in the single-particle approximation. The fact that the correction is directly proportional to the integral over the small component was first found by Margenau [32].

In the general case the g_j factor is evaluated with many-electron wave functions and hence nondiagonal matrix elements are calculated. It is then convenient to rewrite Eq. (12) further.

$$\langle-\beta(2\mathbf{j}-\boldsymbol{l})\rangle=-\langle 2\mathbf{j}\rangle-\langle(\beta-1)2\mathbf{j}-\beta\boldsymbol{l}\rangle. \tag{14}$$

For an s state the nonrelativistic result $g_j=-2$ is thus given by the first term and the two remaining terms will give the bound-state corrections. The second term gives contributions of order α^2 without any large cancellations. The last term, the $\beta\boldsymbol{l}$ operator, mixes states with different j but the same l value . In the nonrelativistic limit the expectation value of $\beta\boldsymbol{l}$ is zero for any s-state since it has rank-one in the orbital space. In a relativistic calculation the contributions from states with different j values but the same l value for the large component will cancel to leading order leaving only contributions of order α^2. However, only the correlation part of the calculation will be affected by these cancellations and the numerical uncertainty always connected with large cancellations has therefore a limited effect on the total uncertainty.

A. Contributions from negative-energy states

Let us now turn our attention to the last term in Eq. (10). The commutator would be zero for the local Coulomb potential $V_{ij}=e/(4\pi\epsilon_0 r_{ij})$. As is well known, such a potential cannot be used to construct a relativistic many-body Hamiltonian. The normal procedure is instead to construct the *no-pair Hamiltonian* with the Coulomb potential projected onto positive-energy states, i.e., surrounded with projection operators. Then the the last commutator in (10) will no longer disappear. However, the result of such a projection onto positive-energy states is that negative-energy states are completely neglected, but negative-energy solutions represent positron states which have to be included properly. We will see that the contributions from the last commutator in (10) when projection operators are inserted around the Coulomb interaction will, to leading order, be canceled by positron contributions. Similar situations have previously been shown to arise also for other operators [31, 33]

First note that the original operator for the interaction with a magnetic field, Eq. (1), is nondiagonal with respect to the large and small component of the relativistic wave function. As an example of how this will affect the perturbation expansion consider the addition of a second perturbation, e.g., the Coulomb interaction with an other electron. As illustrated in Fig. 1(b) it is then possible to get an admixture of negative-energy eigenstates to the unperturbed Hamiltonian. Due to the nondiagonal nature of the operator (1), Fig. 1(b) will contribute in order $\alpha^2 Z$ and due to the non-existence of nonrelativistic bound states corrections the contributions to δg_j from Fig. 1(a) are of the same order. Thus negative- and positive-energy states are equally important. This

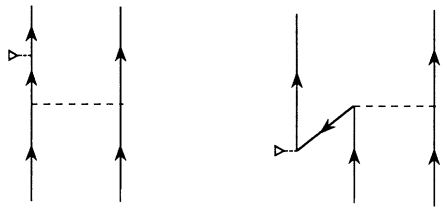

FIG. 1. Diagrams that illustrate the situation when two perturbations are taken into account. The line with a triangle in one end represents the interaction with the magnetic field and the other line represents the Coulomb interaction. Diagram (a) corresponds to the inclusion of positive-energy intermediate states (up-going line), as defined by the eigenstates to the unperturbed Hamiltonian, and diagram (b) corresponds to negative-energy states (down-going line). Due to the nondiagonal nature of operator (1), which describes the interaction with the magnetic field, diagram (b) will contribute to the g_j factor in order $\alpha^2 Z$. Due to the nonexistence of nonrelativistic bound-state corrections, the contributions to δg_j from diagram (a) are of the same order. Thus negative- and positive-energy states are equally important, which is true for the whole perturbation expansion of (1).

is an unusual situation which arises when a completely relativistic phenomenon is described by a nondiagonal operator. The conclusion is thus that in the case of the original operator, Eq. (1), an error in order α^2 will be made if the negative-energy eigenstates to h, Eq. (3), are neglected in the perturbation expansion.

Consider now the last commutator in Eq. (10) and the question of how it will enter in a correct treatment of the negative-energy states. The commutator will be examined when the expectation value is taken between eigenstates to the projected Hamiltonian and afterwards positron contributions will be considered. The relativistic Hamiltonian (2) with a Coulomb potential projected onto positive eigenstates of h is written

$$H = \sum_i h_i + \frac{e^2}{4\pi\epsilon_0} \sum_{i<j} \lambda_i^+ \lambda_j^+ \frac{1}{r_{ij}} \lambda_i^+ \lambda_j^+. \tag{15}$$

The projection operators λ^+ are defined to give zero when operating on negative-energy states but unity when applied to positive energy states. The last term on the right-hand side of Eq. (10) can now be written

$$\frac{e}{2mc}\left[\beta_i \boldsymbol{\alpha}_i \cdot \mathbf{A}_i, \lambda_i^+ \lambda_j^+ \frac{e^2}{4\pi\epsilon_0 r_{ij}} \lambda_i^+ \lambda_j^+\right]$$

$$= \frac{e}{2mc}\Bigg\{ -\lambda_j^+ \left[\beta_i \boldsymbol{\alpha}_i \cdot \mathbf{A}_i, \lambda_i^-\right] \frac{e^2}{4\pi\epsilon_0 r_{ij}} \lambda_i^+ \lambda_j^+ + \lambda_i^+ \lambda_j^+ \frac{e^2}{4\pi\epsilon_0 r_{ij}} \left[\lambda_i^-, \beta_i \dot{\boldsymbol{\alpha}}_i \cdot \mathbf{A}_i\right] \lambda_j^+ \Bigg\}, \tag{16}$$

where the fact that $1/r_{ij}$ commutes with $\beta\boldsymbol{\alpha}\cdot\mathbf{A}$ has been used as well as the relation

$$\lambda^+ + \lambda^- = 1.$$

When an expectation value of Eq. (16) is taken between eigenstates to (15) the contributions

$$\frac{e}{2mc} \sum_{s^-} \left\langle \Psi^{++} \left| \frac{e^2}{4\pi\epsilon_0 r_{ij}} \right| s_i^- \right\rangle \langle s_i^- \mid \beta_i \boldsymbol{\alpha}_i \cdot \mathbf{A}_i \mid \Psi^{++} \rangle + \text{H.c.} \tag{17}$$

are added, where $\mid s_i^- \rangle$ denotes a negative-energy state. The presence of a Hermitian-conjugate term, arising from the first term on the right-hand side of Eq. (16), is indicated in (17). Since $\beta\boldsymbol{\alpha}\cdot\mathbf{A}$ is anti-Hermitian it enters with opposite overall sign.

Now the hitherto neglected contributions from the creation of virtual electron-positron pairs have to be considered. This corresponds to the addition of terms

$$\sum_{s^-} \frac{\langle \Psi^{++} \mid \frac{e^2}{4\pi\epsilon_0 r_{ij}} \mid s_i^- \rangle \langle s_i^- \mid ce\boldsymbol{\alpha}_i \cdot \mathbf{A}_i \mid \Psi^{++} \rangle}{\Delta E} + \text{H.c.} \tag{18}$$

The energy denominator in Eq. (18) will be approximately $2mc^2$. The only effect that the presence of the β matrix in (17) has on the leading-order contributions is a change of, which can easily be seen by examining (17) in detail. Thus contributions from Eq. (18) are, to order α^2, equal but opposite in sign to the contributions from Eq. (17) and they will cancel each other.

The whole discussion above is due to the definition of positive- and negative-energy states in terms of the Hamiltonian h. If instead the definition was made from the Hamiltonian $h + h^m$, neither the contributions (18) nor the nonzero result in Eq. (16) would appear. Figures 1(a) and 1(b) would then be calculated as expectation values of the Coulomb interaction with magnetically perturbed orbitals. Obviously a magnetically perturbed orbital with positive energy includes admixtures from negative as well as positive-energy eigenstates to the Hamiltonian without external fields. This is due to the fact that the whole sum is required to form a complete set.

The conclusion is then that Eq. (12) can safely be used between eigenstates to the Hamiltonian (15) and the last commutator in Eq. (10) disregarded as long as only Coulomb interaction is considered.

B. Contributions from the Breit interaction

Consider again the original operator Eq. (1). As mentioned this operator is non-diagonal with respect to the large and small components of the wave function. This is also true for the Breit interaction

$$B_{ij} = -\frac{e^2}{4\pi\epsilon_0} \frac{1}{2} \left\{ \frac{\boldsymbol{\alpha}_i \cdot \boldsymbol{\alpha}_j}{r_{ij}} + \frac{(\boldsymbol{\alpha}_i \cdot \mathbf{r}_{ij})(\boldsymbol{\alpha}_j \cdot \mathbf{r}_{ij})}{r_{ij}^3} \right\}, \tag{19}$$

which is included in the two-particle term eV_{ij} in Eq. (2). The combination of the magnetic interaction, Eq. (1), and the Breit interaction, Eq. (19), will then contribute in order α^2 provided negative energy states, as defined by h, are considered. These contributions can be written

$$\sum_{s^-} \frac{\langle \Psi^{++} \mid B_{ij} \mid s_i^- \rangle \langle s_i^- \mid ce\boldsymbol{\alpha}_i \cdot \mathbf{A}_i \mid \Psi^{++} \rangle}{\Delta E} + \text{H.c.} \tag{20}$$

As in Eq. (18) ΔE is approximately $2mc^2$ and the whole expression is of order α^2. Contributions from positive-energy states could of course also be added though they will only contribute in order α^4. Although negative-energy eigenstates to h appear in Eq. (20), the use of the Breit interaction in the low-energy limit is justified. This is because it will effectively be evaluated between positive eigenstates to $h + h^m$, although, as was discussed in Sec. II A, negative- as well as positive-energy eigenstates to h are needed to express them. A more detailed discussion can be found in Ref. [34].

In Eq. (10) the magnetic interaction operator, Eq. (1), was rewritten in terms of a commutator with the Hamiltonian and an effective operator. To continue that approach the presence of the Breit interaction in the Hamiltonian has to be considered and additional terms are expected to enter in the effective operator. These new terms will be found when $-eV_{ij}$ in the last commutator on the

right-hand side of (10) is identified with B_{ij}. The commutator will now be examined, but instead of evaluating it explicitly a sum over all states

$$1 = \sum_{\text{all}} | s\rangle\langle s | \tag{21}$$

is inserted between the operators. Note that only the negative-energy states s^- contribute in order α^2. The leading contributions to the commutator are then

$$-\sum_{s^-} \frac{\langle \Psi^{++} | B_{ij} | s_i^-\rangle\langle s_i^- | ce\beta_i\boldsymbol{\alpha}_i \cdot \mathbf{A}_i | \Psi^{++}\rangle}{2mc^2} + \text{H.c.} \tag{22}$$

The denominator ΔE in Eq. (20) is approximately $2mc^2$ and the β matrix in Eq. (22) introduces a change of sign in the leading-order contributions. Thus the results from Eq. (22) and (20) are equal to order α^2 and either can be used to calculate the effect of the Breit interaction. In the calculations presented in Secs. III and IV we have evaluated the effects of the Breit interaction directly as in Eq. (20). The contributions to the g_j factor originating from the Breit interaction corresponds to the diamagnetic terms in nonrelativistic calculations.

C. Radiative effects

When radiative processes are taken into account the interaction between the atom and the external magnetic field is affected in several ways. The most important is the addition of a term

$$h^m_{\text{AMM}} = \frac{e\hbar}{2m}\left(\frac{\alpha}{2\pi} - \cdots\right)\beta\boldsymbol{\sigma}\cdot\mathbf{B} \tag{23}$$

to the expression for the interaction between the atom and the magnetic field, Eq. (1). The expression in parentheses is the anomalous part of the magnetic moment (AMM) for a free electron as found by Schwinger. Equation (23) is exactly of the same form as the spin-dependent term in Eq. (11) and can be treated together with that term. The free-particle Dirac result $g_{\text{Dirac}} = -2$ as well as the bound-state corrections are affected in relative order α. There is no similar correction to the l-dependent term. As was pointed out by Hegstrom [6] this has the effect that the anomalous part does not follow the Dirac part and when the bound-state corrections are calculated it is then not permitted to simply replace the free-particle Dirac results $g_{\text{Dirac}} = -2$ with the experimental value. The lowest-order contributions to the bound-state corrections when Eq. (23) is considered is 3×10^{-8} for Ba^+ and Be^+ and 1×10^{-8} for Li. Since this is below the experimental uncertainty and since there are also other bound-state corrections of radiative origin of similar magnitude, see below, no bound-state radiative corrections are included in this study, but an estimate of their possible contribution is included in the theoretical error estimate.

Second, several terms, which contribute to the Lamb shift, will be added to the Hamiltonian without external fields when radiative processes are taken into account and these may indirectly affect the interaction with an external magnetic field. Consider first the terms which contain the anomalous magnetic moment. The most important of these can be written [35]

$$h_{\text{AMM}} = \frac{e\hbar}{2m}\left(\frac{\alpha}{2\pi} - \cdots\right)\beta\boldsymbol{\alpha}\cdot[\mathbf{p}, V] \tag{24}$$

and the expectation value of the magnetic interaction term in Eq. (1) is changed in order α^3 when evaluated with wave functions which include the effect of (24). This can be seen from the commutator with the full Hamiltonian which was used in (10) to obtain the effective Hamiltonian. When the contribution (24) is added to the Hamiltonian an extra term will appear on the right-hand side of Eq. (10):

$$\delta h^m_{\text{AMM}} = -2i\left(\frac{e}{2mc}\right)^2\left(\frac{\alpha}{2\pi} - \cdots\right)\boldsymbol{\sigma}\cdot(\mathbf{A}\times[\mathbf{p}, V])\,. \tag{25}$$

To examine the order of magnitude of Eq. (25) it is convenient to consider the nuclear part of the potential only. When Eq. (4) is used for $\mathbf{A}$ it is then possible to write

$$\delta h^m_{\text{AMM}} = -\frac{1}{2mc^2}\left(\frac{\alpha}{2\pi} - \cdots\right)\left(-\frac{e}{4\pi\epsilon_0}\frac{Z}{r}\right) \times\frac{e\hbar}{2m}\left\{\boldsymbol{\sigma}\cdot\mathbf{B} - \frac{(\boldsymbol{\sigma}\cdot\mathbf{r})(\mathbf{r}\cdot\mathbf{B})}{r^2}\right\}. \tag{26}$$

The first term in Eq. (26) is the Schwinger correction multiplied with the ratio between the potential and $2mc^2$ times the nonrelativistic result. With hydrogenlike functions this is easily evaluated to $3\times10^{-8}\,(Z/n)^2$ relative to the nonrelativistic g_j factor, where n is the principal quantum number. This is one order of magnitude smaller than the present experimental accuracy for lithium and a factor of 3 smaller than the accuracy for Be^+. Also for Ba^+ this effect is considerably smaller than the experimental error when Z is replaced with a realistic estimate of the Z_{eff} acting on the $6s$ electron. The presence of the contribution in Eq. (25) was originally discussed in [5].

Further, the possibility for corrections to g_j factors originating from self-energy and vacuum-polarization graphs should be considered. These have been studied by Hegstrom [6], who found that no such contributions exist for s states.

III. METHOD OF CALCULATION

The calculation is essentially performed in three steps. First a wave function, an approximation of an eigenstate to the Hamiltonian (15), is constructed using the coupled-cluster single- and double-excitation approach, which is briefly described below. With this wave function the bound-state corrections to the g_j factor are evaluated directly by invoking operator (12) and the procedure for removing the nonrelativistic result which is indicated in Eqs. (13) and (14). The two next steps are due to the effects of the Breit interaction which was penetrated in Sec. II B. The contributions that are to be considered are shown in Eq. (20). The first of these steps is to calculate

the zeroth-order wave function with the Dirac-Fock-Breit (DFB) [34] approximation rather than with the Dirac-Fock (DF) approximation and the perturbation expansion of the Coulomb electron-electron interaction in the CCSD approach is then made from this starting point. Operator (7) is then evaluated with the two approaches and the difference is one important contribution to the g_j factor from Eq. (20). The last step is to include the Breit interaction, Eq. (19), in the CCSD expansion. Earlier this has been done in [24–26] where the Breit interaction was added to the Coulomb electron-electron interaction in Eq. (15), which implies that the two-particle operators are projected onto positive-energy states. Since the order α^2 contributions to the g_j factor from the Breit interaction comes from Eq. (20), care must be taken to include also negative-energy states and ensure that correct energy denominators enter in the diagrams which are to be included in the matrix-elements calculation. This is further discussed in Sec. III B.

A. Wave functions

The wave functions used in the calculation of the matrix elements of the operators (7), (12), and (14) were obtained using the CCSD approach, in which the exact wave function $|\Psi\rangle$ is written in terms of a zeroth-order wave function $|\Psi^0\rangle$ and a cluster operator S as

$$|\Psi\rangle = \{\exp(S)\}\,|\Psi^0\rangle, \tag{27}$$

where the curly brackets denote normal ordering with respect to the occupied states [36]. We use intermediate normalization, i.e., $\langle\Psi \mid \Psi^0\rangle = \langle\Psi^0 \mid \Psi^0\rangle = 1$. The cluster operator is separated into n-body parts

$$S = S_1 + S_2 + \cdots \tag{28}$$

and is, in the case of CCSD, truncated after double excitations. The implementation of the CCSD scheme used here is described in [14]. The graphical equivalent of (28) is shown in Fig. 2. The S_2 cluster includes only excitations into positive-energy eigenstates of the zeroth-order Hamiltonian to avoid spurious contributions from the vacuum. For the S_1 cluster, however, the contributions which involve negative-energy states enter with correct energy denominators and have been included in the calculation. Although many physical effects are only negligibly affected by negative-energy states, they are essential to obtain the correct contributions to the g_j factor from the Breit interaction as was discussed in Sec. II B.

For Li and Be^+ the single- and two-particle clusters were evaluated in a spatial grid containing 91 points. The grid size dependence was checked and found to be insignificant for the numbers of figures given in Sec. IV. The two-particle clusters were then treated by the use of pairfunctions as described by Mårtensson [37] and Lindgren and Morrison [21]. The spherical expansion of the Coulomb and the Breit interaction was truncated after $k_{\max} = 6$. Also the extrapolation of k values gives negligible contributions.

For the substantially larger system Ba^+ it was necessary to introduce certain approximations. In Fig. 3 all core electrons are included in the second-order counterpart of the diagrams, except for the diagrams in Figs. 3(m) and 3(n). However, the interactions between the n=1, 2, and 3 electrons and the other core electrons were neglected in the iteration scheme as well as in the rather unimportant diagrams in Figs. 3(m) and 3(n). This approximation was checked by isolating the inner core-core contributions to the diagram in Fig. 3(a) and these were found to amount to only 3% of the whole diagram, i.e., 0.2% of the total result. The clusters were evaluated in a spatial grid containing 71 points, but the largest contributions, Fig. 3(a) and the lowest-order contributions to Fig. 3(e), were calculated with more grid points. Both for the Breit interaction and the Coulomb interaction between the core electrons the spherical expansion of the electron-electron interaction was trun-

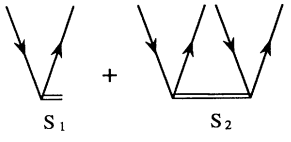

FIG. 2. The diagrammatic representation of the CCSD approximation. The cluster operators S_1 and S_2 represent the one- and two-particle interactions, respectively.

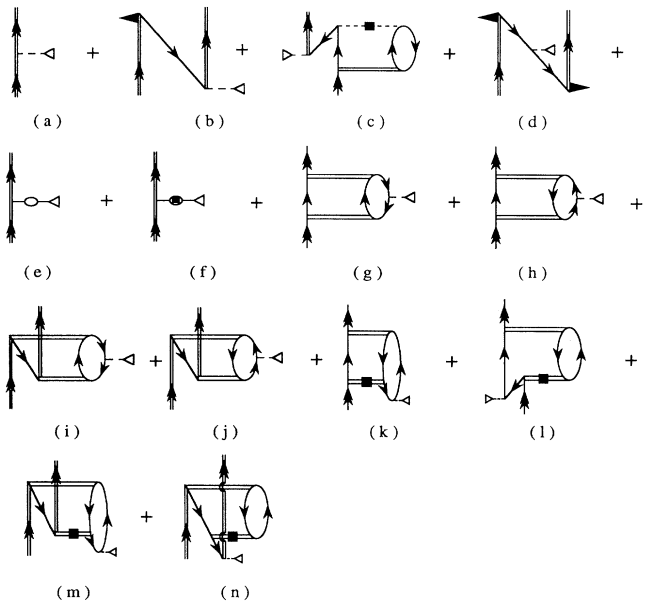

FIG. 3. The leading terms of the expression (29) for a one-particle operator and a one-valence system, using the definitions of Fig. 4. The line with a triangle in one end represents the interaction with the magnetic field and the filled box denotes that the Breit interaction, Eq. (19), is included in the cluster operators. Hermitian conjugates and exchange versions are not shown. Up-going lines with single (double) arrows denote excited (valence) states. Down-going lines denote hole states.

cated after $k_{\max} = 2$. This limit was also used for the interaction between the valence electron and the $n = 1$ and 2 electrons. For the $n = 3$, 4 and 5 shells the core-valence interaction was truncated after $k_{\max} = 3$, 4, and 5, respectively. The truncations may introduce an uncertainty of as much as 10% of the correlation contribution, but has a rather limited effect on the total uncertainty as will be discussed below.

B. Matrix elements

The relativistic version of the procedure described by Mårtensson-Pendrill and Ynnerman [18] was employed to evaluate the matrix elements of the operators (12) and (7). The expression for a matrix element of an operator O using the coupled-cluster wave functions is given by

$$\frac{\langle \Psi_f^0 \mid \left\{\exp\left(S_f^\dagger\right)\right\} O \left\{\exp\left(S_i\right)\right\} \mid \Psi_i^0\rangle}{\langle \Psi_f^0 \mid \left\{\exp\left(S_f^\dagger\right)\right\}\left\{\exp\left(S_f\right)\right\} \mid \Psi_f^0\rangle^{1/2} \langle \Psi_i^0 \mid \left\{\exp\left(S_i^\dagger\right)\right\}\left\{\exp\left(S_i\right)\right\} \mid \Psi_i^0\rangle^{1/2}}. \tag{29}$$

The denominator in (29) is due to the use of non-normalized wave functions. The leading terms of this expression in the case of a one-valence system and a one-particle operator is shown in Fig. 3. In Fig. 3(a) the DFB contribution is included, through the use of DFB orbitals [34], as well as the effect of the S_1 cluster for the valence orbital; see Fig. 4(a). In Figs. 3(b) and 3(d) the contributions from the S_1 cluster for the core orbitals are represented. The Breit interaction is included in the diagram in Fig. 3(c), in which the down-going orbital line represents a negative-energy orbital, leading to contributions of order α^2 for this diagram. In Figs. 3(e) and 3(f) the definitions in Figs. 4(b) and 4(c) are used to obtain the contributions from the random-phase approximation (RPA) as well as some diagrams from the correlation subclass of diagrams. In Fig. 3(f) the Breit interaction and the g_j operator are connected via a negative-energy orbital, which as in Fig. 3(c) enhances the order of magnitude of the contribution. The appearance of negative-energy eigenstates, in terms of the DF Hamiltonian, was discussed in Sec. II B, where it was pointed out that the Breit interaction is effectively evaluated between positive energy eigenstates to $h^{\mathrm{DF}} + h^m$. The diagrams in Figs. 3(g)–3(j) give the correlation contributions from the Coulomb interaction and in the diagrams in Figs. 3(k)–3(n) the Breit interaction has been added to the S_2 cluster in the last interaction. Just as in Fig. 3(c) the down-going orbital next to the g_j operator is of negative-energy character and this class of diagrams therefore contribute in order α^2.

IV. RESULTS

The results are displayed in Table I. The interesting number to compare with experiment is the bound-state correction to the g_j factor which for an S state is obtained as the difference between the experimental value for the atomic system and the free-particle value $g_s = -2.002\ 319\ 304\ 377(9)$. The lithium result, which is described in [38], is a combination of three different experiments measuring the ratio of the g_j factors for lithium and potassium, potassium and rubidium, and rubidium and the free electron, respectively. The error for the bound-state correction is dominated by a 10% uncertainty for $g_j(\mathrm{Li})/g_j(\mathrm{K}) - 1$, resulting in an overall uncertainty of 3%. The present result for Li is in close agreement with the calculation in the nonrelativistic limit by Veseth [10]. The Be^+ and Ba^+ measurements are both ion-trap experiments. The former experiment by Wineland, Bollinger, and Itano [39–41] derived the g_j value for the ground state from hyperfine measurements

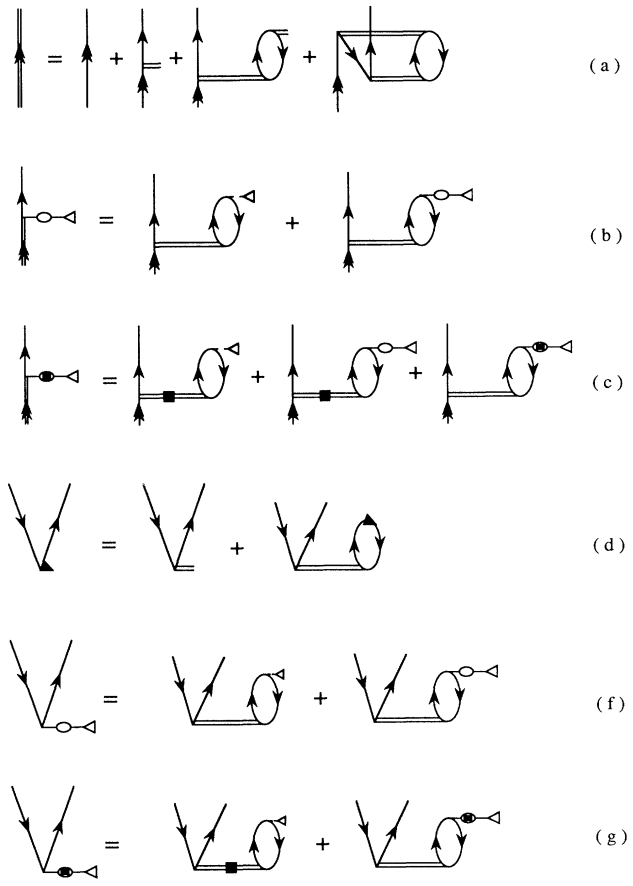

FIG. 4. Graphical definitions of the modification of orbital lines and effective interactions, which facilitates the inclusion of infinite chains of diagrams in the matrix-element calculations. The filled box in (c) and (g) denote that the Breit interaction is included in the cluster operators.

TABLE I. Contributions to the bound-state corrections to the g_j factor from the diagrams in Fig. 3. The corrections are relative to the free-electron value $g_s = -2.002\,319\,304\,377(9)$ and obtained as $\delta g = g_j - g_s$. The results are displayed as $10^5 \delta g$. The numbers in parentheses are the contributions added to the result for each diagram when the perturbation expansion is performed with a Dirac-Fock-Breit basis set rather than with eigenstates to the Dirac-Fock Hamiltonian.

Correction	Li		Be^+		Ba^+	
Dirac-Fock	1.4198	(−0.0500)	4.8086	(−0.1235)	6.25	(0.71)
Fig. 3(a) DF	0.0451	(0.0019)	0.0745	(0.0047)	0.27	(−1.23)
Fig. 3(b)	−0.0013	(0.0001)	−0.0031	(0.0002)	−0.18	(0.09)
Fig. 3(c)	0.1820		0.2685		1.81	
Fig. 3(d)	0.0000	(0.0000)	0.0000	(0.0000)	−0.04	(−0.04)
Fig. 3(e) "first order"	0.1850	(−0.0132)	0.4401	(−0.0221)	−26.10	(0.47)
Fig. 3(e) "higher orders"	0.0083	(−0.0005)	0.0139	(−0.0006)	0.10	(−0.00)
Fig. 3(f) "first order"	0.1352		0.3271		0.89	
Fig. 3(f) "higher orders"	0.0141		0.0242		−0.07	
Fig. 3(g)	−0.0031	(−0.0088)	−0.0004	(−0.0111)	6.57	(0.17)
Fig. 3(h)	−0.0046	(−0.0075)	−0.0020	(−0.0076)	−8.24	(−3.43)
Fig. 3(i)	0.0000	(0.0000)	0.0000	(0.0000)	−1.39	(−0.06)
Fig. 3(j)	0.0018	(−0.0035)	0.0049	(−0.0040)	−0.30	(−0.13)
Fig. 3(k)	−0.0028		0.0006		0.02	
Fig. 3(l)	−0.2204		−0.3168		−2.18	
Fig. 3(m)	−0.0006		−0.0009		0.00	
Fig. 3(n)	0.0001		0.0023		0.02	
Norm	0.0137	(0.0146)	0.0120	(0.0142)	5.38	(5.05)
Total	1.772±0.020		5.653±0.050		−17.18±0.3	
Experiment	1.831±0.064[a]		5.694±0.033[b]		−17.13±0.12[c]	

[a]Derived from measurements of the quotas $\frac{g_j(\mathrm{Li})}{g_j(\mathrm{K})}$, $\frac{g_j(\mathrm{K})}{g_j(\mathrm{Rb})}$, and $\frac{g_j(\mathrm{Rb})}{g_s}$ as reviewed by Arimondo, Inguscio, and Violino in [38].
[b]Wineland, Bollinger, and Itano [41].
[c]Knab *et al.* [2].

with an estimated error of 0.9%. The g_j factor for Ba^+ has been measured by the Mainz group using two different methods. A derivation of the Zeeman splitting of each level from measurements of the $6s_{1/2}, m - 6p_{1/2}, m'$ transitions [1] resulted in rather large error bars, but a later experiment where optical pumping and an induced microwave resonance were used [2] gave a several order of magnitude better result: $g_{\mathrm{exp}} - g_s = -17.13(12) \times 10^{-5}$.

The contributions from each diagram, and its exchange counterpart, in Fig. 3 are displayed in Table I. The contributions added to each diagram when the perturbation expansion is made with a Dirac-Fock-Breit basis set rather than with eigenstates to the Dirac-Fock Hamiltonian are separated out and given in parentheses. For Ba^+ these contributions to Figs. 3(a) and 3(h) and to the normalization may seem rather large. However, added together the diagrams beyond the RPA-like diagrams, i.e., Figs. 3(a), 3(b), 3(d), and 3(g)–3(j) and the normalization, get an extra contribution of only 0.089 when the Dirac-Fock basis set is replaced by the Dirac-Fock-Breit basis set, as can be seen on the seventh line in Table II. The large contributions for individual diagrams are an artifact due to the use of non-normalized wave functions; cf. (29). The diagrams Figs. 3(c), 3(f), and 3(k)–3(n) are due to the inclusion of the Breit interaction in the perturbation expansion. The contributions from different classes of diagrams are summarized in Table II.

For both Li and Be^+ around 95% of the final result is given by the sum of the Dirac-Fock value and the diagrams illustrated in Fig. 3(e), which are dominated by RPA-like diagrams. The entries "first order" and "higher orders" correspond to the first and second diagram in Fig. 4b. Correlation beyond the RPA-like diagrams contribute with 3% and 1.5%, respectively, and the total effect of the Breit interaction is 1.6% for Li and 2.3% for Be^+. For Ba^+ the situation is very different. The lowest-order result even shows the wrong sign. After inclusion of the RPA chains, which are completely dominated by the polarization of the $5p$ orbitals, the result is 20% above the experimental result. The remaining contributions come from the Breit interaction and the correlation due to the Coulomb interaction which contribute with 10% each of the final result.

The theoretical uncertainties are estimated contributions from radiative corrections, which are probably less than 1% as discussed in Sec. II C, the pure numerical uncertainty and the uncertainty caused by the truncation of the spherical expansion of the two-particle interactions, discussed in Sec. III A. For Li and Be^+ the latter is small since all contributions with $k_{\mathrm{max}} \leq 6$ were included. The lowest-order result is in addition the dominant contribution and higher-order effects show a stable behavior.

TABLE II. Contributions to the bound-state corrections to the g_j factor from different classes of diagrams. The corrections are relative to the free-electron value $g_s = -2.002\ 319\ 304\ 377(9)$ and obtained as $\delta g = g_j - g_s$. The results are displayed as $10^5 \delta g$.

Correction	Li	Be^+	Ba^+
Lowest order, Dirac-Fock	1.470	4.932	5.539
Δ Dirac-Fock-Breit	−0.050	−0.124	0.708
RPA-like diagrams	0.207	0.477	−26.455
Δ Dirac-Fock-Breit	−0.014	−0.023	0.462
Breit RPA-like diagrams	0.149	0.351	0.824
Coulomb correlation	0.055	0.090	1.985
Δ Dirac-Fock-Breit	−0.003	−0.004	0.089
Breit correlation	−0.042	−0.046	−0.330
Total	1.772±0.020	5.653±0.050	−17.18±0.3
Experiment	1.831±0.064[a]	5.694±0.033[b]	−17.13±0.12[c]

[a]Derived from measurements of the quotas $\frac{g_j(\mathrm{Li})}{g_j(\mathrm{K})}$, $\frac{g_j(\mathrm{K})}{g_j(\mathrm{Rb})}$, and $\frac{g_j(\mathrm{Rb})}{g_s}$ as reviewed by Arimondo, Inguscio, and Violino in [38].
[b]Wineland, Bollinger, and Itano [41].
[c]Knab *et al.* [2].

An estimated uncertainty of a few percent in the many-body part of the calculation gives an overall uncertainty of around 0.1%. Thus an estimated error of 1% should not be too optimistic. The behavior of Ba^+ is considerably less stable. The lowest-order result has the wrong sign and the situation is restored only after inclusion of RPA effects. Since Ba^+ is a rather large system it was necessary to use some approximations as was discussed in Sec. III A. We assume that the overall uncertainty due to numerical uncertainties and truncations in the CCSD scheme could lead to an error of around 1%. To account also for possible radiative contributions we estimate the total error to 2%.

V. CONCLUSIONS

The present calculation shows that the CCSD approach can give accurate results for the bound-state corrections to atomic g_j factors. The importance of correlation as well as effects due to the Breit interaction are demonstrated, particularly for the heavy many-electron system Ba^+. At present the experimental accuracy is on the limit to probe bound-state radiative contributions. The theoretical treatment of these contributions will be an interesting challenge for the future.

ACKNOWLEDGMENTS

This work has benefited from the help of several colleagues. Early-stage discussions with Jean-Louis Heully provided background material and inspiration. The continuous support and invaluable assistance from Ann-Marie Mårtensson-Pendrill is greatly acknowledged. Discussions with Ingvar Lindgren and Sten Salomonson have been fruitful and improved the scientific clarity. Professor G. Werth is acknowledged for help on the comparison with experimental data. Financial support was received from the Swedish Natural Science Research Council (NFR).

* Electronic address: f3aeva@fy.chalmers.se
† Electronic address: f3aay@fy.chalmers.se

[1] A. Hubrich, H. Knab, K. H. Knöll, and G. Werth, Z. Phys. D **18**, 113 (1991).
[2] H. Knab, K. Knöll, F. Scheerer, and G. Werth, Z. Phys. D (to be published).
[3] W. M. Itano, J. C. Bergquist, and D. J. Wineland, J. Opt. Soc. Am. B **2**, 1392 (1985).
[4] R. A. Hegstrom, Phys. Rev. **184**, 17 (1969).
[5] H. Grotch and R. A. Hegstrom, Phys. Rev. **4**, 59 (1971).
[6] R. A. Hegstrom, Phys. Rev. **7**, 451 (1973).
[7] H. Grotch and R. A. Hegstrom, Phys. Rev. **8**, 1166 (1973).
[8] R. A. Hegstrom, Phys. Rev. **11**, 421 (1975).
[9] L. Veseth, Phys. Rev. **22**, 803 (1980).
[10] L. Veseth, J. Phys. B **16**, 2891 (1983).
[11] V. A. Dzuba, V. V. Flambaum, P. G. Silvestrov, and O. P. Sushkov, Phys. Scr. **31**, 275 (1985).
[12] V. A. Dzuba, V. V. Flambaum, P. G. Silvestrov, and O. P. Sushkov, Phys. Rev. A **44**, 2828 (1991).
[13] V. V. Flambuam, I. B. Khriplovich, and O. P. Sushkov, Phys. Lett. **67A**, 177 (1978).
[14] S. Salomonson and P. Öster, Phys. Rev. A **41**, 4670 (1990).
[15] S. Salomonson and P. Öster, Phys. Rev. A **40**, 5559 (1989).
[16] S. Salomonson and P. Öster, Phys. Rev. A **40**, 5548 (1989).
[17] W. R. Johnson, S. Blundell, and J. Sapirstein, Phys. Rev. A **37**, 307 (1988).

[18] A.-M. Mårtensson-Pendrill and A. Ynnerman, Phys. Scr. **41**, 329 (1990).
[19] S. Salomonson and A. Ynnerman, Phys. Rev. A **43**, 88 (1991).
[20] A.-M. Mårtensson-Pendrill, L. Pendrill, S. Salomonson, A. Ynnerman, and H. Warston, J. Phys. B **23**, 1749 (1990).
[21] I. Lindgren and J. Morrison, *Atomic Many-Body Theory, Series on Atoms and Plasmas*, 2nd ed. (Springer-Verlag, New York, 1986).
[22] I. Lindgren, Phys. Rev. A **31**, 1273 (1985).
[23] I. Lindgren, Rep. Prog. Phys. **47**, 345 (1984).
[24] E. Lindroth and S. Salomonson, Phys. Rev. A **41**, 4659 (1990).
[25] E. Lindroth, H. Persson, S. Salomonson, and A.-M. Mårtensson-Pendrill, Phys. Rev. A **45**, 1493 (1991).
[26] E. Lindroth and J. Hvarfner, Phys. Rev. A **45**, 2771 (1991).
[27] A. Hartley, E. Lindroth, and A.-M. Mårtensson-Pendrill, J. Phys. B **23**, 3417 (1991).
[28] A. Hartley and A.-M. Mårtensson-Pendrill, Z. Phys. D **15**, 309 (1991).
[29] A. Hartley and A.-M. Mårtensson-Pendrill, J. Phys. B **24**, 1193 (1991).
[30] P. G. H. Sandars, J. Phys. B **1**, 511 (1968).
[31] E. Lindroth, B. W. Lynn, and P. G. H. Sandars, J. Phys. B **22**, 559 (1989).
[32] H. Margenau, Phys. Rev. **57**, 383 (1940).
[33] J. Hiller, J. Sucher, G. Feinberg, and B. Lynn, Ann. Phys. (N.Y.) **127**, 149 (1980).
[34] E. Lindroth, A.-M. Mårtensson-Pendrill, A. Ynnerman, and P. Öster, J. Phys. B **22**, 2447 (1989).
[35] H. A. Bethe and E. E. Salpeter, in *Quantum Mechanics of One- and Two-Electron Atoms* (Plenum, New York, 1977), p. 96.
[36] I. Lindgren, Int. J. Quantum Chem. S**12**, 33 (1978).
[37] A.-M. Mårtensson, J. Phys. B **12**, 3995 (1979).
[38] E. Arimondo, M. Inguscio, and P. Violino, Rev. Mod. Phys. **49**, 31 (1977).
[39] D. J. Wineland, J. J. Bollinger, and W. M. Itano, Phys. Rev. Lett. **50**, 628 (1983).
[40] D. J. Wineland, J. J. Bollinger, and W. M. Itano, Phys. Rev. Lett. **50**, 1333(E) (1983).
[41] The result $g_j = -2.002\ 262\ 36(31)$ is obtained from Ref. [39] when the most recent values for the mass ratios; $m_p/m_e = 1836.152\ 701(37)$ and $m(^9\mathrm{Be}^+)/m_p = 8.946\ 534\ 45(41)$ are used.